Hydrogen bonding interaction of methyl-substituted pyridines with thioacetamide: Steric hindrance of methyl group

ARTICLE *in* CHEMICAL PHYSICS LETTERS · SEPTEMBER 2001

Impact Factor: 1.9 · DOI: 10.1016/S0009-2614(01)00844-2

14 September 2001

ELSEVIER

Chemical Physics Letters 345 (2001) 338–344

CHEMICAL PHYSICS LETTERS

www.elsevier.com/locate/cplett

Hydrogen-bonding interaction of methyl-substituted pyridines with thioacetamide: steric hindrance of methyl group

Kee-Hyun Choi [a], Ho-Jin Lee [a], Alfred Karpfen [b], Chang-Ju Yoon [c], Jeunghee Park [d,*], Young-Sang Choi [a,*]

[a] *Department of Chemistry, Korea University, 1 Anamdong Seoul, 136-701 Republic of Korea*

[b] *Institut fuer Theoretische Chemie und Molekulare Strukturbiologie, Universitaet Wien A-1090 Wien, Waehringer Strasse 17, Austria*

[c] *Department of Chemistry, The Catholic University of Korea, Pucheon, 420-743 Republic of Korea*

[d] *Department of Chemistry, Korea University, 208 Seochangdong Jochiwon, 339-700 Republic of Korea*

Received 29 May 2001; in final form 11 July 2001

Abstract

The hydrogen-bonding interaction between a series of methyl-substituted pyridines as proton acceptors and thioacetamide as a proton donor in CCl_4 has been investigated using near-infrared absorption spectroscopy. The stability of the 1:1 hydrogen-bonded complex increases with the number of methyl groups and depends on the position of methyl groups. The steric hindrance of ortho-methyl groups particularly reduces the stability of complex. The relative stability agrees with the ease of miscibility of pyridines with water for methyl and dimethyl homologs. The calculated proton affinities and the DFT association energies using 6-31+G(d, p) and 6-311++G(2d, 2p) basis sets reveal the steric hindrance of ortho-methyl groups.

1. Introduction

Since pyridine derivatives are common proton acceptors of hydrogen bonding in biological system, a quantitative account of their hydrogen-bonding interactions is essential to parameterize accurate mechanical force fields for molecular modeling [1–3]. In addition, the binary liquid mixture alkyl-substituted pyridine–water has gained considerable interest due to its drastic change in miscibility depending on the number, size, and position of alkyl groups [4–11]. Various models have been proposed to explain the unique immiscibility gap in the phase diagram using the structure of interacting molecules [7–10]. Recently, Pápai and Jancsó [11] calculated the hydrogen-bonding interaction energies for the methyl-substituted pyridine–water complexes in the gas phase. They showed that a methyl substituent stabilizes the hydrogen bonding, and the degree of stabilization varies with the number and position of methyl groups. But they concluded that the computed association energies are not correlated well with the miscibility behaviors of pyridine series. Despite such interests in the hydrogen-bonding interaction between alkyl-substituted pyridine and water, there are a few experimental works to verify the role of alkyl group in the hydrogen bonding of pyridine molecules [12].

* Corresponding author. Fax: +82-2-3290-3992.

E-mail addresses: parkjh@tiger.korea.ac.kr (J. Park), yschoi@korea.ac.kr (Y.-S. Choi).

0009-2614/01/$ - see front matter
PII: S0009-2614(01)00844-2

In the present work, we investigate the effect of methyl-substituents on the hydrogen-bonding interaction of pyridine with thioacetamide (TA) in CCl_4. We choose TA as a proton donor for methyl-substituted pyridines and employed a near-infrared (NIR) spectroscopic technique. Methyl-substituted pyridines are pyridine (Py), 2-methylpyridine (2-MPy), 3-methylpyridine (3-MPy), 4-methylpyridine (4-MPy), 2,4-dimethylpyridine (2,4-DMPy), 3,4-dimethylpyridine (3,4-DMPy), 2,6-dimethylpyridine (2,6-DMPy), and 2,4,6-trimethylpyridine (2,4,6-TMPy). The NIR spectroscopic technique we used in this work has provided very accurate measurements of thermodynamic parameters for the hydrogen-bonding formation of TA with various proton acceptors [13–16]. In order to understand the hydrogen-bonding ability of methyl-substituted pyridine molecules, we calculated their proton affinities (PAs) and the association energies of the hydrogen-bonded complexes for Py, 2-MPy, and 4-MPy.

2. Methodology

2.1. Experimental section

Py (Aldrich, 99.8%), 2-MPy (Aldrich, 98%), 3-MPy (Aldrich, 99%) 4-MPy (Aldrich, 99%), 2,4-DMPy (Aldrich, 99%), 3,4-DMPy (Aldrich, 98%), 2,6-DMPy (Aldrich, 99%), 2,4,6-TMPy (Aldrich, 99%), and CCl_4 (J.T. Baker, HPLC grade) were dried by adding 4 Å molecular sieves (Aldrich) without further purification. TA (Aldrich, 99%) was dried at room temperature under a reduced pressure ($\sim 10^{-2}$ Torr) for 24 h, and stored in an argon-filled glove box. The molar concentration ratio of TA (2.0–6.0 mM) to methyl-substituted pyridines in CCl_4 was 1:30. All samples were prepared in the glove box.

The NIR absorption spectrum of TA/pyridine/CCl_4 solution in a 1-cm path-length quartz cell was measured using a Cary 5G UV–VIS-NIR spectrophotometer (Varian). Since we are interested in the NIR absorption band of TA, the absorption due to pyridine and CCl_4 was eliminated by placing a matching cell containing an equal concentration of pyridine in the path of reference beam. The sample and reference cells were placed in a multi-cell holder (Varian) connected to a temperature controller (Varian). The temperature range was 283–318 K and temperature fluctuation during the measurement was less than ± 0.1 K. The cell compartment was purged by nitrogen gas passing through calcium chloride, in order to remove the humidity. The baseline was always corrected in each measurement. The *Peak Fit* (AISN Software) program was used for the non-linear least square fitting of the NIR absorption band by a Gaussian–Lorentzian product function. The program terminates its iteration when χ^2 was less than 1×10^{-7}.

2.2. Computational section

Computations were carried out using the GAUSSIAN 98 program [17]. The geometries were fully optimized using HF, B3LYP (DFT), and MP2 methods with the 6-31G(d) basis set [18–22]. The harmonic vibrational frequencies were calculated at the same levels by means of analytical second-derivative techniques to evaluate the corresponding zero point energies (ZPEs). PA is defined as negative value of enthalpy change for $B(g) + H^+(g) \rightarrow BH^+(g)$ reaction. For evaluating the absolute PA value the following equation was used [23]:

$$\mathrm{PA(B)} = -\Delta E^0_{\mathrm{elec}} - \Delta \mathrm{ZPE} + \Delta E_{\mathrm{vib}}(T) + \frac{5}{2}RT,$$

where $\Delta E^0_{\mathrm{elec}}$ represents the difference between the electronic energies of products and reactants at 0 K, ΔZPE is the difference in zero-point energies of BH^+ and B, $\Delta E_{\mathrm{vib}}(T)$ accounts for the change in population of vibrational levels at temperature T, and the last term incorporates the classical correction for translation ($\frac{1}{2}RT$ per degree of freedom), rotation ($\frac{1}{2}RT$ per degree of freedom), and the conversion factor of energy to enthalpy (ΔnRT).

The DFT association energies for 1:1 TA:Py, TA:2-MPy, and TA:4-MPy complexes were calculated at the B3LYP/6-31+G(d, p) and B3LYP/6-311++G(2d, 2p) levels of theory [20–22]. The influence of the basis set superposition error (BSSE) has been evaluated with the aid of conventional counterpoise (CP) procedure including

the influence of geometry relaxation upon complex formation [24].

3. Results and discussions

3.1. Thermodynamic parameters for hydrogen-bonded complex formation of methyl-substituted pyridines with TA in CCl_4

The v^{as}_{N-H} + amide II combination band of TA was chosen because of the large absorption coefficient and little interference from other peaks [13–16]. The v^{as}_{N-H} + amide II combination bands of 6.0 mM TA with 180 mM pyridine in CCl_4 at various temperatures are shown in Fig. 1a. The peaks at 1968 nm (5081 cm^{-1}) and 1978 nm (5056 cm^{-1}) are assigned to monomeric TA and hydrogen-bonded TA, respectively. As the temperature increases, the absorption intensity of the monomer band increases, but that of the dimer band decreases. The spectra show an isosbestic point, which indicates the equilibrium of only two species, monomeric and hydrogen-bonded TA. In the temperature range between 283 and 318 K, the formation of 1:2 hydrogen-bonded complexes was not found. Each of the monomeric and hydrogen-bonded TA absorption bands is well fitted by a Gaussian–Lorentzian product function, as shown in Fig. 1b. The sum of the two band areas is independent of temperature within experimental error, indicating that the integrated absorption coefficients of monomer and hydrogen-bonded complex bands are the same. The detailed data analysis procedure was described in our previous works [15].

The equilibrium of hydrogen-bonded complex formation and its equilibrium constants (K) are expressed by the following equations:

$$\begin{aligned} &\mathrm{TA} + \mathrm{acceptor} \rightleftharpoons \mathrm{TA:acceptor}, \\ &K = C_{1:1}/C_{\mathrm{mono}}C_{\mathrm{free}}, \quad C_{1:1}/C_{\mathrm{mono}} = C_{\mathrm{free}}K. \end{aligned} \tag{1}$$

Here, $C_{1:1}$ is the concentration of the hydrogen-bonded TA, C_{mono} is the concentration of monomeric TA, and C_{free} is the concentration of the free proton acceptors. The ratio of $C_{1:1}$ to C_{mono} is obtained directly from the area of the two resolved bands, since the integrated absorption coefficients of the two bands are the same. The linear fit of the $C_{1:1}/C_{\mathrm{mono}}$ vs. C_{free} plot yields the equilibrium constant (K). As an approximation, instead of the activity, the concentration was used. Table 1 lists the equilibrium constants for the formation of the 1:1 hydrogen-bonded complex in the temperature

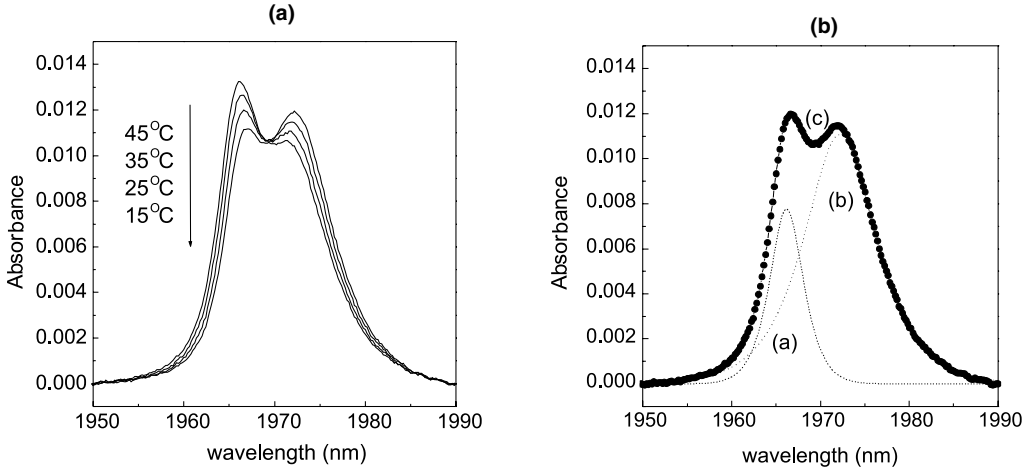

Fig. 1. (a) The v^{as}_{N-H} + amide II combination band of 6.0 mM TA with 180 mM Py in CCl_4 at 288, 298, 308, and 318 K, showing an isosbestic point. (b) The computer resolved v^{as}_{N-H} + Amide II of 6.0 mM TA with 180 mM Py in CCl_4, at 298 K. Filled circles (•••), dashes (- - -), and dots (···) represent measured absorption spectrum, resolved monomeric band, and hydrogen-bonded complex band, respectively.

Table 1
Thermodynamic parameters for 1:1 TA:methyl-substituted pyridine hydrogen-bonded complex formation in CCl_4 solution

Proton donor	Proton acceptor	Equilibrium constant (M^{-1})				ΔH^0 (kcal/mol)	ΔS^0 (cal/mol K)
		288 K	298 K	308 K	318 K		
TA	Py	18.1 ± 0.9	13.9 ± 0.7	11.3 ± 0.6	8.6 ± 0.4	-4.5 ± 0.1	-9.9 ± 0.2
	2-MPy	18.8 ± 0.9	14.5 ± 0.7	10.3 ± 0.5	8.3 ± 0.4	-5.0 ± 0.1	-11.7 ± 0.1
	3-MPy	27.6 ± 1.4	20.3 ± 1.0	15.4 ± 0.8	12.9 ± 0.6	-4.6 ± 0.1	-9.6 ± 0.2
	4-MPy	31.8 ± 1.6	22.3 ± 1.1	16.3 ± 0.8	13.5 ± 0.7	-5.2 ± 0.1	-11.2 ± 0.1
	2,4-DMPy	25.8 ± 1.3	19.9 ± 1.0	14.7 ± 0.7	10.4 ± 0.5	-5.9 ± 0.1	-13.9 ± 0.1
	3,4-DMPy	45.7 ± 2.3	32.2 ± 1.6	23.0 ± 1.2	18.3 ± 0.9	-5.7 ± 0.1	-12.1 ± 0.2
	2,6-DMPy	11.7 ± 0.6	9.2 ± 0.5	6.8 ± 0.3	5.3 ± 0.3	-4.6 ± 0.1	-11.0 ± 0.2
	2,4,6-TMPy	18.6 ± 0.9	13.6 ± 0.7	9.9 ± 0.5	7.0 ± 0.4	-5.6 ± 0.1	-13.8 ± 0.2

range 283–318 K. The equilibrium constants at 298 K are 13.9, 14.5, 20.3, and 22.3 M^{-1} for Py, 2-MPy, 3-MPy, and 4-MPy, respectively, in the order Py < 2-MPy < 3-MPy < 4-MPy. 2-MPy forms a hydrogen-bonded complex with TA less efficiently than other methyl pyridines. The K values at 298 K for 2,4-DMPy, 3,4-DMPy, 2,6-DMPy, and 2,4,6-TMPy are 19.9, 32.2, 9.2, and 13.6 M^{-1}, respectively. 2,6-DMPy and 2,4,6-TMPy show smaller K values than Py.

Using the van't Hoff equation, i.e., $d(\ln K)/d(1/T) = -\Delta H^0/R$, the standard enthalpy change (ΔH^0) values and the standard entropy change (ΔS^0) values are obtained from the plots of $R \ln K$ vs. $1/T$ as shown in Fig. 2 and are listed in Table 1.

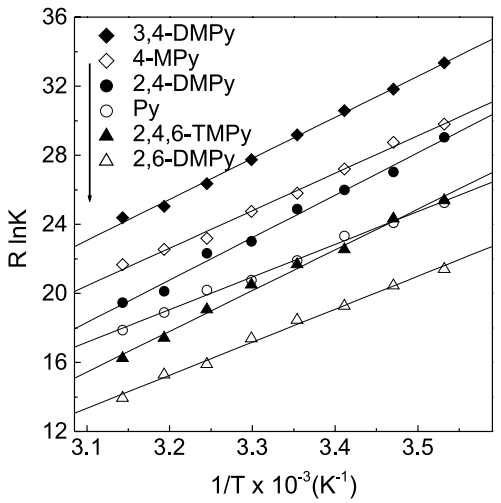

Fig. 2. A plot of $R \ln K$ vs. $1/T$ for the formation of 1:1 TA:pyridine hydrogen-bonded complexes.

When a methyl group substitutes 2- and 4-positions of pyridine, the $-\Delta H^0$ value increases by 0.5 and 0.7 kcal/mol, respectively. In the case of 3-MPy, the increase of the $-\Delta H^0$ value due to the substitution of a methyl group is 0.1 kcal/mol, which is less than those of 2-MPy and 4-MPy. This result can be rationalized by the resonance and/or inductive effect of methyl group at 2- and 4-positions. The smaller $-\Delta H^0$ value of 2-MPy than that of 4-MPy results from the steric hindrance of the ortho-methyl group. The ΔH^0 value of 2,6-DMPy is almost similar to that of Py, showing that the steric hindrance effect becomes more significant as the methyl groups substitute 2- and 6-positions of pyridine. Due to the resonance and/or inductive effect of methyl group at 4-postition, the $-\Delta H^0$ values of 2,4- and 3,4-DMPy are larger than those of 2-MPy and 3-MPy. But the $-\Delta H^0$ value of 2,4,6-TMPy is smaller than those of 2,4-DMPy and 3,4-DMPy because of two ortho-methyl groups.

3.2. Hydrogen bond strength vs. miscibility of pyridine with water

The size of the immiscibility gaps in the phase diagram of pyridine–water solutions shows a wide variation depending on the number, size, and position of alkyl substituents. The relationship between the miscibility and the hydrogen bond strength has been a subject of controversy [7–11]. Many studies suggest that the immiscibility gap shrinks upon increasing the hydrogen bond strength [7–9]. A more recent study, however, shows that the immiscibility gap is extended when strengthening the hydrogen bonds [10].

The ease of miscibility follows a sequence of pyridine > methylpyridines > dimethylpyridines. In the methylpyridine series, the sequence is given by 4-MPy > 2-MPy > 3-MPy. The sequence is 2,4-DMPy $\sim 3,4$-DMPy $> 2,6$-DMPy for the dimethylpyridine series. We found that within the mono- and di-methyl homologs of pyridine the $-\Delta H^0$ values of the hydrogen-bonded complexes with TA are in the same sequence as the ease of miscibility with water. Therefore, we suggest that in mono- and di-methyl homologs of pyridine the strengthening of the hydrogen bond can enhance the miscibility extent of pyridine with water. However, the increase of the immiscibility gap with the number of methyl groups is not simply explained by our $-\Delta H^0$ values, suggesting that other typed interactions such as hydrophobic interaction, etc. would also involve in determining the miscibility property of pyridine molecules in aqueous solution. The agreement of our experimental results with the miscibility behavior of mono- and di-methyl substituted pyridines reveal unequivocally that the ortho-methyl group inhibits the hydrogen-bonding interaction toward both proton donors TA and water.

3.3. Correlation with proton affinity

Since it was reported that the PA could reflect the hydrogen-bonding ability or basicity for certain molecules [25–27], we performed ab initio calculations of PA using DFT and MP2 methods. Table 2 shows the calculated PA values of the pyridine series at the nitrogen atom site using DFT (B3LYP) and MP2 methods with 6-31G(d) basis set. The ΔPA values represent the PA values relative to that of Py. The calculated and available experimental ΔPA values show a good correlation with $R^2 = 0.9966$ for DFT and $R^2 = 0.9939$ for MP2 [28]. This indicates that the increase of PA values due to the methyl substituents is described well with the MP2 and DFT calculations.

The $-\Delta H^0$ values of the TA:pyridine hydrogen-bonded complex formation vs. the calculated PA values using DFT method are plotted in Fig. 3. 2,6-DMPy and 2,4,6-TMPy exhibit a significant deviation from a linear correlation (shown as a line in Fig. 3). This plot provides a robust evidence for the strong steric hindrance of the ortho-methyl groups toward the hydrogen-bonding formation with TA.

Table 2
Theoretical PA and experimental PA

Molecules	Calculated ΔPA (kcal/mol)[a]		Experimental ΔPA[b] (kcal/mol)
	MP2/6-31G(d)	B3LYP/6-31G(d)	
Py	0.0 (221.0)[c]	0.0 (224.5)[c]	0.0 (222.0)[c]
2-MPy	3.9	4.6	4.6
3-MPY	3.2	3.3	3.5
4-MPy	3.8	4.4	4.4
2,4-DMPy	7.4	8.7	8.1
3,4-DMPy	6.6	7.3	6.8
2,6-DMPy	7.5	8.7	8.2
2,4,6-TMPY	10.7	12.4	

[a] Relative PA values to that of Py.
[b] Ref. [28].
[c] Absolute values of Py.

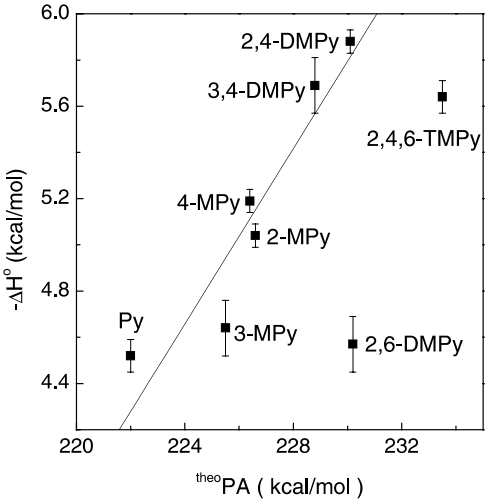

Fig. 3. A plot of the standard formation enthalpy change ($-\Delta H^0$) of TA:pyridine hydrogen-bonded complexes vs. calculated PA (^{theo}PA) values using DFT (B3LYP)/6-31G(d) method. The data excluding 2,6-DMPy and 2,4,6-TMPy are linearly fitted.

3.4. DFT association energies of 1:1 TA:Py, TA:2-MPy, and TA:4-MPy complexes

The association energies of the TA:Py, TA:2-MPy, and TA:4-MPy hydrogen-bonded complexes

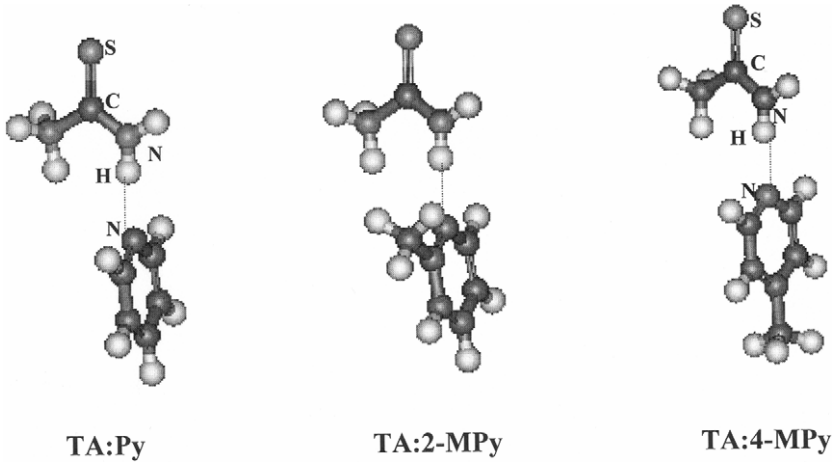

Fig. 4. The equilibrium structure of TA:Py, TA:2-MPy, and TA:4-MPy complexes at the B3LYP/6-311++G(2d, 2p) level.

were calculated at the B3LYP/6-31+G(d, p) and B3LYP/6-311++G (2d, 2p) levels. The geometry of the complexes was only optimized for the case that the *anti*-H of TA forms the intermolecular hydrogen bonding with the nitrogen of pyridine. The association energies calculated with the B3LYP/6-31+G(d, p) basis set are −7.18, −7.09, and −7.59 kcal/mol for the Py, 2-MPy, and 4-MPy complexes, respectively. With the 6-311++G(2d, 2p) basis set, the association energies without the BSSE correction are −6.56, −6.50, and −6.98 kcal/mol for Py, 2-MPy, and 4-MPy, respectively. With the BSSE correction, the respective values are −6.34, −6.24, and −6.74 kcal/mol. The calculation clearly demonstrates that the hydrogen-bonding ability of 2-MPy is less than that of 4-MPy, which is consistent with the experimental result. Fig. 4 displays the geometries of TA:Py, TA:2-MPy, and TA:4-MPy complexes calculated at the B3LYP/6-311++G(2d, 2p) level. The distance between the H atom of TA and the N atom of the pyridine ring is 2.033, 2.020, and 2.019 Å, respectively, for Py, 2-MPy, and 4-MPy (see Table 3).

Pápai and Jancsó calculated the association energy of 1:1 methyl-substituted pyridine–water complexes with the aid of B3LYP (DFT) and MP2 methods [11]. For Py, 2-MPy, 3-Mpy, 4-MPy, and 2,6-DMPy, the DFT association energies increase in the order Py < 2, 6-DMPy < 2-MPy < 3-MPy < 4-MPy while the MP2 association energies follow the order Py < 4-MPy < 3-MPy < 2-MPy < 2, 6-MPy. Their DFT association energies predict the diminished hydrogen-bonding interaction of 2-MPy and 2,6-DMPy with water due to the steric hindrance of ortho-methyl group, which is incorporated in our experimental results. The MP2 association energies apparently overestimate the dispersion interaction of the ortho-methyl group. It is remarkable that the DFT method can predict the relatively weak hydrogen-bonding interaction of ortho-methyl substituted pyridine molecules.

Table 3
The DFT association energies (kcal/mol) of 1:1 TA:Py, TA:2-MPy, and TA:4-MPy hydrogen-bonded complexes

Complexes	B3LYP/ 6-31+G(d, p)	B3LYP/ 6-311++G(2d, 2p)
TA:Py	−7.18	−6.56 (−6.34)[a]
TA:2-MPy	−7.09	−6.50 (−6.24)[a]
TA:4-MPy	−7.59	−6.98 (−6.74)[a]

[a] w/BSSE.

4. Conclusions

We have measured the thermodynamic data for the hydrogen-bonded complex formation of methyl-substituted pyridines such as Py, 2-MPy, 3-MPy, 4-MPy, 2,4-DMPy, 3,4-DMPy, 2,6-DMPy, and 2,4,6-TMPy with TA in CCl_4 by employing NIR spectroscopic technique. The standard enthalpy change ($-\Delta H^0$) generally increases with the

number of methyl groups, which results from the resonance and/or inductive effect of methyl group. However, the methyl group at ortho-position exhibits a steric hindrance toward the hydrogen-bonding interaction with TA. There is a correlation between the $-\Delta H^0$ values and the miscibility extent with water for methyl- and di-methyl substituted pyridine series. It indicates that the miscibility of methyl-substituted pyridine series with water increases with the hydrogen-bonding strength at least within mono- and di-methyl homologs. The steric hindrance of the ortho-methyl group can inhibit the hydrogen-bonding interaction with water. The PA values calculated by DFT and MP2 methods show a good correlation with available experimental PA values. 2,6-DMPy and 2,4,6-TMPy exhibits a strong deviation behavior from a linear relationship of $-\Delta H^0$ values with the PA values, because of the sterically hindered ortho-methyl groups. The DFT association energies of 1:1 TA:Py, TA:2-MPy, and TA:4-MPy using 6-31+G(d, p) and 6-311++G(2d, 2p) basis sets show that 2-MPy forms a less stable hydrogen-bonded complex compared to 4-MPy, which is consistent with our experimental results.

Acknowledgements

This work was supported by the Basic Science Research Institute program funds (BSRI-99-3405, BSRI-99-3432). Some of the calculations were performed on the Cluster of Digital Alpha Servers (2100 4/275 and 5/375) of the computer center of the University of Vienna. The authors are grateful for ample supply of computer time on this installation.

References

[1] P. Chakrabarti, U. Samanta, J. Mol. Biol. 251 (1995) 9.
[2] U. Samanta, P. Chakrabarti, J. Chandrasekhar, J. Phys. Chem. A 102 (1998) 8964.
[3] P. Hobza, M. Kabelac, J. Sponer, P. Mejzlik, J. Vondrasek, J. Comput. Chem. 18 (1997) 1136.
[4] R.J.L. Andon, J.D. Cox, J. Chem. Soc. 1952 (1952) 4601.
[5] J.D. Cox, J. Chem. Soc. 4606 (1952).
[6] R.J.L. Andon, J.D. Cox, E.F.G. Herington, Trans. Faraday Soc. 53 (1957) 410.
[7] R.E. Goldstein, J.S. Walker, J. Chem. Phys. 78 (1983) 1492.
[8] J.S. Walker, C.A. Vause, J. Chem. Phys. 79 (1983) 2660.
[9] R.E. Goldstein, J. Chem. Phys. 79 (1983) 4439.
[10] I.V. Brovchenko, A.V. Oleinikova, J. Chem. Phys. 106 (1997) 7756.
[11] I. Pápai, G. Jancsó, J. Phys. Chem. A 104 (2000) 2132 (and references therein).
[12] M. Tamres, S. Searles, E.M. Leighly, D.W. Mohrman, M. Tamres, J. Am. Chem. Soc. 76 (1954) 3983.
[13] Y.S. Choi, Y.D. Huh, O.D. Bonner, Spectrochim. Acta A 41 (1985) 1127.
[14] B.K. Min, H.-J. Lee, Y.S. Choi, J. Park, C.-J. Yoon, J.-A. Yu, J. Mol. Struct. 471 (1998) 283.
[15] N.-K. Kim, H.-J. Lee, K.-H. Choi, J.-A. Yu, C.-J. Yoon, J. Park, Y.-S. Choi, J. Phys. Chem. A 104 (2000) 5572.
[16] K.-Y. Kim, H.-J. Lee, A. Karpfen, J. Park, C.-J. Yoon, Y.-S. Choi, Phys. Chem. Chem. Phys. 3 (2001) 1973.
[17] M.J. Frisch, et al., GAUSSIAN 98, Revision A.7, Gaussian, Inc., Pittsburgh, PA, 1998.
[18] G.A. Petersson, A. Bennett, T.G. Tensfeldt, M.A. Al-Laham, W.A. Shirley, J. Mantzaris, J. Chem. Phys. 89 (1988) 2193.
[19] G.A. Petersson, M.A. Al-Laham, J. Chem. Phys. 94 (1991) 6081.
[20] A.D. Becke, Phys. Rev. A 38 (1988) 3098.
[21] C. Lee, W. Yang, R.G. Parr, Phys. Rev. B 37 (1988) 785.
[22] E.J. Baerends, O.V. Gristsenko, J. Phys. Chem. 101 (1997) 5383.
[23] M.-C. Ou, S.-Y. Chu, J. Phys. Chem. 99 (1995) 556 (and references therein).
[24] S.F. Boys, F. Bernardi, Mol. Phys. 19 (1970) 553.
[25] P.R. Rablen, J.W. Lockman, W.L. Jorgensen, J. Phys. Chem. A 102 (1998) 3782.
[26] S. Hammerum, T.I. Sølling, J. Am. Chem. Soc. 121 (1999) 6002.
[27] Y. Podolyan, L. Gorb, J. Leszczynski, J. Phys. Chem. A 104 (2000) 7346.
[28] E.P. Hunter, S.G. Lias, J. Phys. Chem. Ref. Data 27 (1998) 413.